

The Nickel Hydroxide Electrode from the Solid-State Chemistry Point of View

C. Delmas, C. Faure, L. Gautier, L. Guerlou-Demourgues and A. Rougier

Phil. Trans. R. Soc. Lond. A 1996 **354**, 1545-1554

doi: 10.1098/rsta.1996.0063

Email alerting service

Receive free email alerts when new articles cite this article - sign up in the box at the top right-hand corner of the article or click [here](#)

To subscribe to *Phil. Trans. R. Soc. Lond. A* go to:
<http://rsta.royalsocietypublishing.org/subscriptions>

The nickel hydroxide electrode from the solid-state chemistry point of view

BY C. DELMAS, C. FAURE, L. GAUTIER, L. GUERLOU-DEMOURGUES AND
A. ROUGIER

*Institut de Chimie de la Matière Condensée de Bordeaux and Ecole Nationale
Supérieure de Chimie et Physique de Bordeaux, Av. Dr Schweitzer,
33608 Pessac Cedex, France*

Our understanding of the behaviour of the nickel hydroxide electrode can be improved significantly by using a solid-state chemistry approach in which knowledge of its structure plays the main role. These studies can be carried out successfully by using relatively well crystallized materials, obtained by 'chimie douce' reactions from high-temperature oxides, which play the role of model materials. The α/γ cycling and the effect of cations substituted for nickel on the electrode behaviour has been characterized in detail.

1. Introduction

The nickel oxide electrode is used as the positive plate of alkaline Ni-Fe, Ni-Zn, Ni-Cd, Ni-H₂ and Ni-MH batteries. The first two systems, although theoretically very promising, are not used practically as their main drawbacks, i.e. bad charge retention and poor cyclability, respectively, have never been overcome in a convenient way. In contrast, the others are used extensively in specific and sophisticated applications. Their high-power density, very good cyclability and specific energy, 50% higher than the lead-acid battery, make them very competitive for an extended range of applications. Strong competition is appearing with the rapid development of the lithium-ion batteries, but they still have a useful future for many years, at least for large systems like electric vehicles.

Although the nickel oxide electrode has been in use for over a century in alkaline batteries, its behaviour is not yet completely understood. A significant improvement in our knowledge of its behaviour has been observed during the last ten years due to the contribution of solid-state chemists who have considered specifically the materials involved in the electrochemical cycling both from a solid-state chemistry and material science point of view, complementing previous work by electrochemists on the macroscopic electrode behaviour (Oliva *et al.* 1982).

The structure of nickel hydroxides and oxyhydroxides consists of NiO₂ slabs, made of edge-sharing NiO₆ octahedra, between which protons, alkali ions, water molecules and even anions can be reversibly intercalated and deintercalated during the electrochemical cycling. Depending on the experimental conditions of the material preparation, the size of the individual slabs and their stacking can vary considerably, leading to a large variety of electrochemical behaviours. The relation between the structure and the composition of the main materials is illustrated schematically by

Phil. Trans. R. Soc. Lond. A (1996) **354**, 1545–1554

Printed in Great Britain

1545

© 1996 The Royal Society

TeX Paper

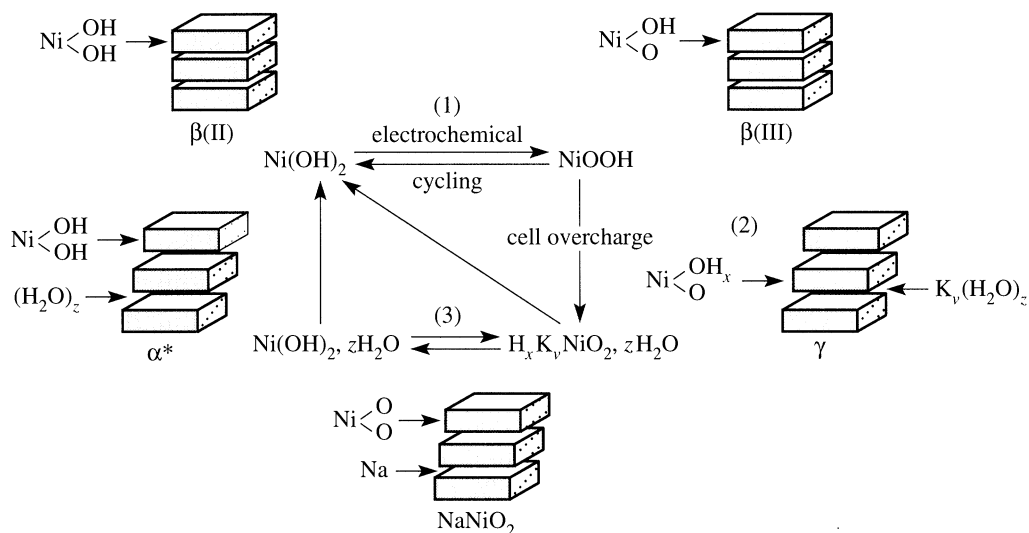


Figure 1. The Bode diagram; comparison of the structure of hydroxides, oxyhydroxides and of sodium nickelate.

the well-known Bode diagram shown in figure 1 (Bode *et al.* 1966). In the first two materials there are no water molecules intercalated between the slabs, while in the other two water intercalation leads to enlarged interslab distances. During a normal cycle, performed using unsubstituted nickel hydroxide ($\text{Ni}(\text{OH})_2$), all four materials are formed successively, at least partially. The oxidation potential of β - $\text{Ni}(\text{OH})_2$ is so close to that of the water decomposition that the cell must be overcharged in order to obtain a large capacity upon discharge; under these conditions a significant amount of the $\beta(\text{III})$ - NiOOH phase is converted into the γ - $\text{H}_x\text{K}_v\text{NiO}_2 \cdot z\text{H}_2\text{O}$ phase, which is the thermodynamically stable oxyhydroxide. At the following cell discharge, the γ -phase leads to an α -phase which is unstable in concentrated KOH and thus gives rise to the classical β - $\text{Ni}(\text{OH})_2$ hydroxide through a dissolution–nucleation–growing mechanism, as shown by the work of Figlarz's group (Le Bihan & Figlarz 1972). The very large interslab distance modifications which occur during these reactions lead rapidly to a degradation of the electrode and, therefore, to a significant decrease in the cell performance. In order to optimize the cycle life of the electrode, numerous studies have been carried out to stabilize either the $\beta(\text{II})/\beta(\text{III})$ system or the α/γ one and therefore suppress all cross reactions. In our laboratory, interest has been focused on the α/γ stabilization, and the main results are reported in this paper.

2. Material preparation and structural characterization

These hydroxides can be obtained either directly by precipitation or by chimie douce reactions from the alkali metal nickelates (Delmas *et al.* 1992).

The classical precipitation method allows one to obtain materials with a very small crystallite size, which is very convenient from the electrochemical point of view, but consequently makes the material characterization difficult.

As shown in figure 1, the structural similarity between NaNiO_2 and the hydroxides and oxyhydroxides allows one to obtain these materials from the sodium nickelate by simultaneous exchange and intercalation reactions without any modification of the NiO_2 slabs. In this case, the large particle size of the precursor phase (synthesized at

The nickel hydroxide electrode

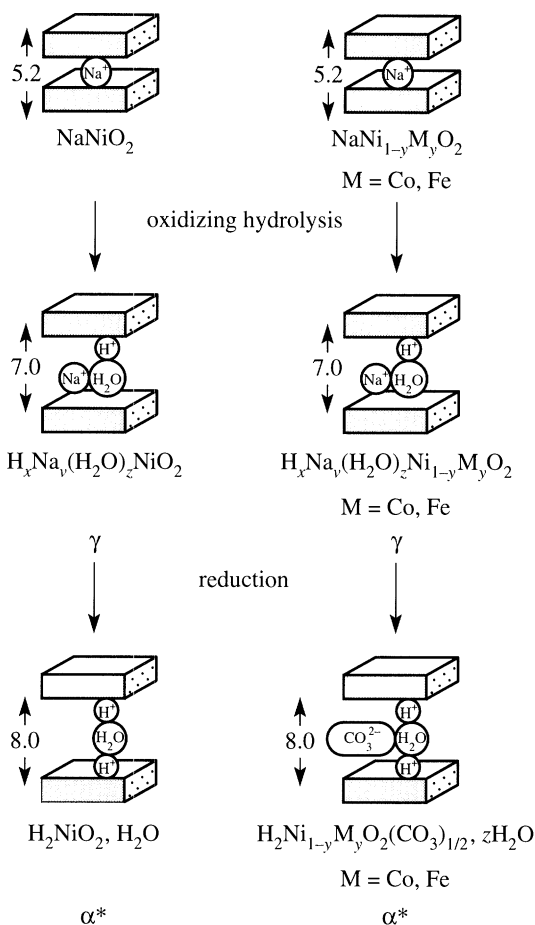


Figure 2. Schematic structure modifications during the 'chimie douce' reactions.

high temperature) is maintained, to a first approximation, during the chimie douce reaction, leading to relatively well crystallized oxyhydroxides and hydroxides. In fact, a slight chemical grinding occurs, as shown clearly by a small broadening of the X-ray diffraction lines. Nevertheless, these materials can be characterized easily by X-ray diffraction and can be considered as model materials to explain the physical and electrochemical behaviour of nickel hydroxides and oxyhydroxides in rechargeable alkaline batteries.

Figure 2 shows schematically the reaction process and structure modifications induced by the chimie douce reactions for the unsubstituted nickel system and for the cobalt- and iron-substituted phases. In both cases, the oxidizing hydrolysis (performed with an $\text{NaClO} + \text{KOH}$ solution) leads to the same γ -type oxyhydroxide with the general formula $\text{H}_{0.2}\text{K}_{0.3}\text{Ni}_{1-y}\text{M}_y\text{O}_2 \cdot (\text{H}_2\text{O})_z$ with $z = 0.50$. It is interesting to note that, whatever the M cation substituted for nickel, the general formula is preserved, with the average oxidation state of Ni + M remaining close to 3.5. This behaviour shows that the general formula for γ -type oxyhydroxides is imposed by the structure rather than by the intrinsic redox properties of the substituting cations. In contrast, the reduction reaction (H_2O_2 solution) leads to significantly different materials. In the case of the unsubstituted nickel system, the reduction leads to a hydrated

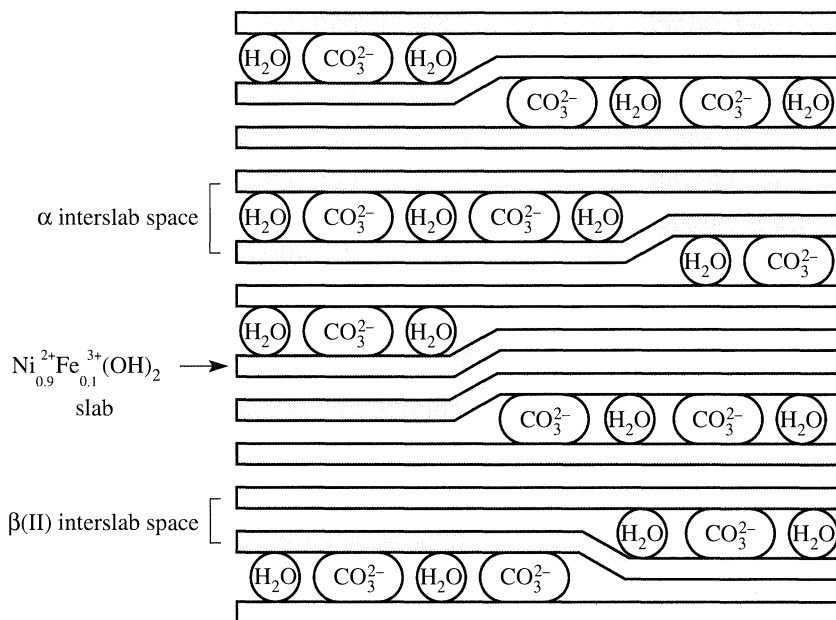


Figure 3. Schematic structure of an interstratified nickel-iron oxyhydroxide.

α^* -hydroxide which, like the homologous α -phase obtained directly by precipitation, is unstable in KOH and gives the β - $\text{Ni}(\text{OH})_2$ phase. In the cobalt- or iron-substituted systems, the reduction reaction leads to divalent nickel and trivalent cobalt or iron within the hydroxides. If y is the degree of substitution, the average oxidation state is therefore equal to $2 + y$. In order to preserve the charge balance, negative species (OH^- , CO_3^{2-} , etc.) must be intercalated into the interslab space. These species are strongly bonded to the slab by ionic bonds and act as pillars to stabilize the structure. The general formula for these hydroxides is $\text{H}_2\text{Ni}_{1-y}\text{M}_y\text{O}_2 \cdot (\text{CO}_3)_{y/2} \cdot (\text{H}_2\text{O})_z$ with $\text{M} = \text{Fe}, \text{Co}$ and $z = 0.50$. These materials are fully stable in concentrated KOH solutions at room temperature. The pillar concentration is directly related to the anion negative charge and to the amount of trivalent cations within the substituted NiO_2 slab; therefore for small amounts of substituting cations, the number of intercalated anions is too small to achieve a full occupancy of the overall interslab space. An anion segregation in some interslab spaces (or in some parts of the interslab spaces) occurs, leading to a interstratified structure with Daumas-Hérol domains, like in the case of graphite intercalated compounds. Figure 3 gives a schematic overview of the slab packing in such an interstratified material. The random distribution of the two types of interslab spaces perpendicular to the slabs prevents the existence of a unit cell; therefore the X-ray diffraction patterns cannot be indexed. Nevertheless, their overall shape can be simulated successfully thanks to statistical methods like those of Hendricks & Teller (1942).

3. Electrochemical behaviour

In the case of the $\beta(\text{II})/\beta(\text{III})$ system, the electrochemical process can be easily described, as only one ionic species (H^+) is involved. However, the process is much more complicated for the α/γ system, since at least four species (H^+ , K^+ , H_2O , OH^- and/or CO_3^{2-}) must be intercalated or deintercalated during the overall reaction.

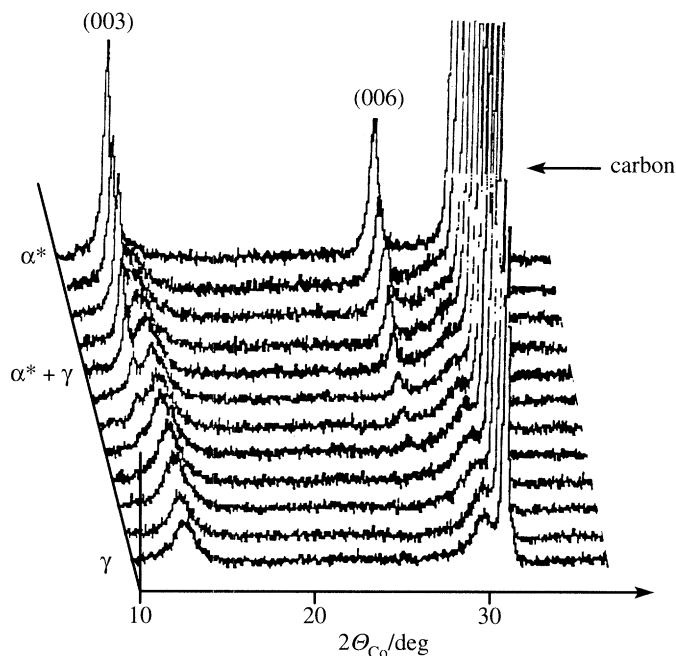


Figure 4. X-ray diffraction pattern modifications of the positive electrode during the second charge of a Ni-Cd cell. This *in situ* experiment has been realized in the $C/10$ regime from a cobalt-substituted nickel hydroxide (α^* type, $y_{Co} = 0.30$).

When the substituted α -type hydroxide is obtained in air by chemical reduction of the γ -type oxyhydroxide, carbonate anions are intercalated; in the case of the electrochemical reduction which occurs during the cell discharge, one can assume that mainly OH^- anions are intercalated.

(a) *In situ* X-ray characterization

In order to gain a better understanding of what is happening during the electrochemical cycling, an *in situ* X-ray diffraction study has been performed during the electrochemical cycling of a Ni-Cd battery with a cobalt-substituted α -hydroxide (30% cobalt substitution). The modifications of the X-ray diffraction patterns during the second charge are illustrated in figure 4. The main results are: (i) the phase diagram consists of two solid solutions separated by a biphased domain; (ii) the homogeneity range of the γ -type solid solution is larger than that of the α -type solution; (iii) a composition hysteresis is observed between charge and discharge; (iv) the thermodynamic cell voltage varies continuously within the two-phase domain; and (v) the reversible broadening of the (001) lines during the charging of the cell emphasizes the more homogeneous charge distribution within the α -phase interslab space relative to the γ -phase. In all experiments only a few cycles were performed, and in no case did the $\beta\text{-Ni}(\text{OH})_2$ phase appear; this point emphasizes clearly the stabilization resulting from the cobalt substitution.

(b) *Long-range cycling*

These cobalt-substituted nickel hydroxides were tested in Ni-Cd cells with 5 M KOH as the electrolyte. In order to emphasize the influence of the particle size on the material stability, the experiments were performed simultaneously on materials

obtained by chimie douce (α^*) and by the classical precipitation method (α) (Delmas *et al.* 1992; Faure *et al.* 1991). Both materials have the same chemical formula except for a larger amount of adsorbed water in the case of the precipitated phase. Figure 5 gives the variation of the number of exchanged electrons (NEE) per Ni + Co versus the number of cycles for two discharge rates, $C/5$ and $5C$. As mentioned previously, the average oxidation state in the γ -phase is close to 3.5, while in the α -phase ($y_{\text{Co}} = 0.3$) it is equal to 2.3. This results in that at most 1.2 electrons per transition element are expected to be reversibly exchanged.

At the lower discharge rate, for materials obtained by chimie douce reactions (α^*), the capacity increases continuously at the beginning of the cycling up to 1.15 electrons, which is very close to the expected theoretical value. The increase at the beginning of the cycling certainly results from the formation of the mosaic structure which is more able to accept the steric constraints than the monolithic one (Delahaye 1986). Although for the material obtained by precipitation (α), the maximum value is reached rapidly after a few cycles. This material exhibits small particles which makes the formation of the mosaic structure easier, or even unnecessary.

The difference in behaviour is much more pronounced at the high discharge rate; in this case, the current density was chosen in order to complete the whole reaction within 12 min. The intrinsic diffusion coefficients of all species which are intercalated and deintercalated during the discharge process are similar in both materials, which differ from one another only by the particle size; this means that in the case of materials obtained by precipitation the reaction is almost complete in a very limited time, while only a part of the intercalation–deintercalation process occurs in the case of materials obtained by chimie douce, which exhibit a significantly larger particle size. At low discharge rate ($C/5$) the particle size of the chimie douce material is not large enough to limit the intercalation–deintercalation process within the allowed reaction time (5 h).

Another interesting point concerns the decrease in the number of exchanged electrons during long-range cycling of the precipitated material at low discharge rate. After more than one hundred cycles, the NEE, the shape of the discharge curve, the voltage at half discharge and the X-ray diffraction show that the α/γ system has been completely converted into the $\beta(\text{II})/\beta(\text{III})$ system. The modification of the derivatives of the discharge curves illustrates clearly the continuous evolution from the α/γ system to the $\beta(\text{II})/\beta(\text{III})$ system. In order to understand why the cobalt-substituted α -type hydroxide is stable indefinitely in 5 M KOH, but not during electrochemical cycling in the same electrolyte, ageing tests at various temperatures and with various KOH concentrations were performed for both types of materials. These experiments show the occurrence of a demixing phenomenon leading to a mixture of $\beta\text{-Ni}(\text{OH})_2$ and CoOOH which is electrochemically inactive. High magnification SEM experiments show that this reaction occurs via a microdissolution and nucleation process which is activated by a higher temperature, higher KOH concentration and smaller particle size. Consequently, the apparent stability during the electrochemical cycling of the materials obtained by chimie douce results from their higher particle size (and may be the more ideal shape for the platelets) which limits considerably the microdissolution. In order to explain why the material obtained by precipitation is completely stable in 5 M KOH but not during the electrochemical process, one has to consider the discharge mechanism, which involves the intercalation of 1.8 protons per Ni + Co atom. Depending on the electrode porosity, the local pH can be considerably increased at the surface of the platelets where the protons are intercalated. Therefore

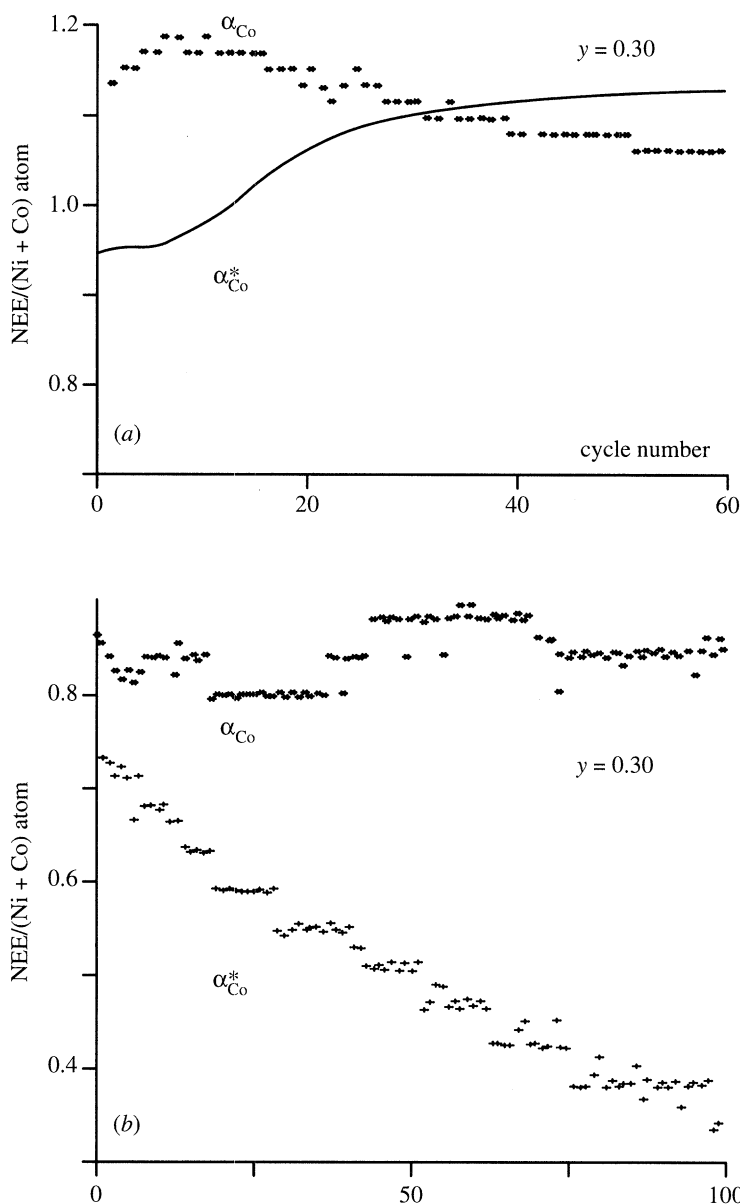


Figure 5. Variation of the number of exchanged electrons during cycling from cobalt-substituted nickel hydroxides obtained either by precipitation (α) or by chimie douce (α^*) ($y_{Co} = 0.30$). The cycling has been realized in (a) the $C/5$ regime or (b) in the $5C$ regime.

the surface of the α -type phase can be a favourable medium for the transformation to the $\beta(II)$ phase via the previously described process.

(c) Cell voltage monitoring

Cationic substitution allows not only the stabilization of the α/γ cycling but also monitoring of the cell voltage. It is well known that cobalt substitution leads to a decrease of the cell voltage, while iron substitution leads to an increase. This behaviour is illustrated in figure 6, which gives the voltage variation during the third

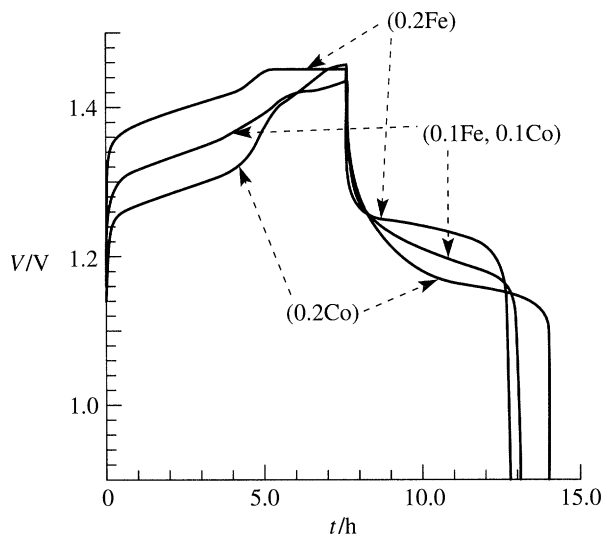


Figure 6. Effect of the substitution ion within the nickel hydroxide on the cell voltage of a Ni-Cd cell.

charge-discharge cycle of Ni-Cd batteries with a substituted α -phase as the positive electrode material: the lowest voltage is observed for the cobalt-substituted phase while the highest is obtained in the case of iron substitution (Guerlou-Demourgues & Delmas 1994). Moreover, for materials substituted with both cobalt and iron, an intermediate voltage value is obtained.

The voltage monitoring is of great interest from the application point of view as it allows one to optimize the cell chargeability. Indeed, the cell potential of the nickel hydroxide oxidation is very close to that of the water oxidation which leads to oxygen evolution. Therefore, both reactions occur simultaneously at the end of the charge, leading to an energy loss as the water decomposition is an irreversible reaction. For applications, a special cell design is required in order to allow the oxygen reduction at the negative plate and therefore makes continuous water addition unnecessary. If the cell voltage is too high, which is primarily interesting from the energy point of view, the main part of the charge energy will be lost to decomposition of the electrolyte; the positive electrode material will not be completely oxidized and therefore a poor capacity will be recovered in discharge even if the cell is strongly overcharged. Moreover, the cell cannot stay in the charged state as the positive electrode material may spontaneously oxidize the electrolyte.

The effect of cationic substitution on the voltage has been studied in detail in the case of mixed Co-Al-substituted α -type nickel hydroxides of general formula $\text{H}_2\text{Ni}_{0.75}\text{Co}_{0.25-t}\text{Al}_t\text{O}_2 \cdot (\text{CO}_3)_{0.125} \cdot (\text{H}_2\text{O})_z$. In this case, the overall substitution rate has been chosen as 0.25 in order to completely stabilize the α/γ system. As shown in figure 7a, aluminium substitution in the pure hydroxide leads to a continuous increase of the half-discharge potential, which must oppose the decrease observed in the case of cobalt substitution. For mixed substituted materials, the voltage can be very precisely monitored, as illustrated in figure 7b, and in this case the cell chargeability can be optimized (Gautier & Delmas 1996).

The voltage modifications induced by the cationic substitution result from the change of the position of the $\text{Ni}^{4+}/\text{Ni}^{3+}$ redox pair in the γ -oxyhydroxide induced by the ligand field at the nickel site. This ligand field, which depends on the Ni-O

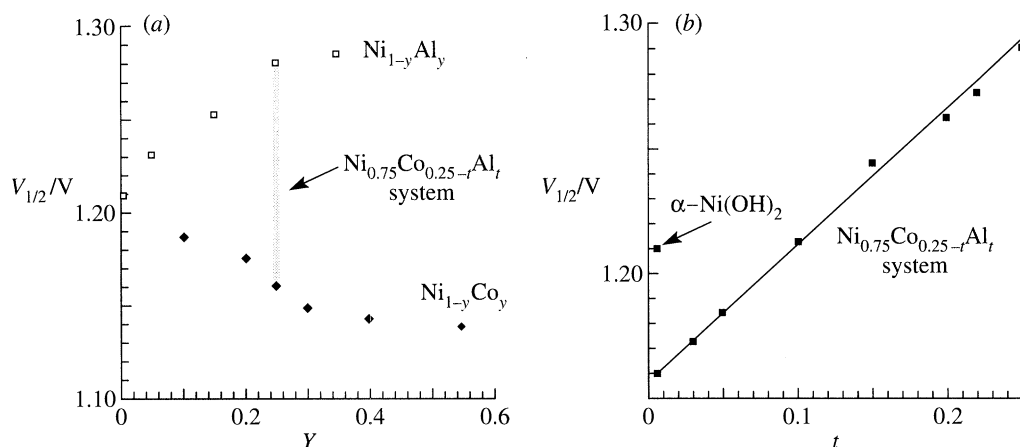


Figure 7. Monitoring of the half-discharge potential of a Ni–Cd cell by cationic substitution within the nickel hydroxide.

distance and on the charge carried by the oxygen anions, can be adjusted by the substitution in the vicinity of the nickel ions of other cations with various ionic radii and electronegativities. In the case of cobalt-substituted γ -oxyhydroxides, the magnetic and electrical properties show the presence of tetravalent nickel while cobalt remains in the trivalent state. In contrast, the magnetic study performed on iron-substituted phases showed that both cations are oxidized simultaneously. Such behaviour has been confirmed by a Mössbauer study, which shows unambiguously the presence of low-spin tetravalent iron (Guerlou-Demourgues 1995). The iron reduction process has been studied by *in situ* Mössbauer spectroscopy experiments, which were realized for the first time during electrochemical cycling of a nickel–cadmium battery. All these results show that the oxidation state distribution results from a compromise between the intrinsic oxidation state stability and the effect on the substituting cation of the ligand field imposed by the prevailing cation within the $\text{Ni}_{1-y}\text{M}_y\text{O}_2$ slab.

4. Conclusion

The study of the nickel hydroxide electrode from the solid-state chemistry point of view provides new insights into its behaviour that complement previous work by electrochemists. The reaction process occurring during the electrochemical cell charge–discharge is a true topotactic intercalation, as in the case of the intensively studied lithium intercalation compounds. The simultaneous presence of a hydroxide and of its precipitating agent (KOH) leads to an equilibrium between the solid phase and the solution, which involves a continuous microdissolution and reprecipitation of the hydroxide, leading to an increase of the particle size and even to segregation phenomena. Therefore, the behaviour of the nickel hydroxide electrode is governed by a solid-state reaction on the time scale of one electrochemical cycle, while it is governed by a solid–solution equilibrium on the time scale of the cell life.

The authors thank M. Ménétrier for fruitful discussions, C. Denage, S. Goma and G. Nabias for technical assistance and CNES, DRET and Région Aquitaine for financial support.

References

- Bode, H., Dehmelt, K. & Witte, J. 1966 *Electrochim. Acta* **11**, 1079.
- Delahaye, A. 1986 Thesis. University of Picardie, Amiens, France.
- Delmas, C., Faure, C. & Borthomieu, Y. 1992 *Mat. Sci. Engng B* **13**, 89.
- Faure, C., Delmas, C. & Willmann, P. 1991 *J. Power Sources* **36**, 497.
- Gautier, L. & Delmas, C. 1996 *J. Power Sources*. (Submitted.)
- Guerlou-Demourgues, L. & Delmas, C. 1994 *J. Electrochem. Soc.* **141**, 713.
- Guerlou-Demourgues, L., Fournés, L. & Delmas, C. 1995 *J. Solid State Chem.* **114**, 6.
- Hendricks, S. B. & Teller, E. 1942 *J. Chem. Phys.* **10**, 147.
- Le Bihan, S. & Figlarz, M. 1972 *J. Cryst. Growth* **13–14**, 458.
- Oliva, F., Leonardi, J., Laurent, J. F., Delmas, C., Braconnier, J. J., Figlarz, M., Fievet, F. & de Guibert, A. 1982 *J. Power Sources* **8**, 229.